Article

Total Bio-Based Material To Fight Cancer Through Antimicrobial Activity

Vincenzo Patamia , Chiara Zagni , Roberto Fiorenza , Sandro Dattilo , Paolo Maria Riccobene , Giuseppe Floresta * , Antonio Rescifina *

Posted Date: 7 June 2023

doi: 10.20944/preprints202306.0502.v1

Keywords: resveratrol; curcumin; halloysite nanotubes; kojic acid; iron chelation, antibacterial.

Article

Total Bio-based Material to Fight Cancer through Antimicrobial Activity

Vincenzo Patamia [1], Chiara Zagni [1], Roberto Fiorenza [2], Sandro Dattilo [3], Paolo Maria Riccobene [3], Giuseppe Floresta [1,*] and Antonio Rescifina [1,*]

[1] Dipartimento di Scienze del Farmaco e della Salute, Università di Catania, Viale A. Doria 6, 95125 Catania, Italy; vincenzo.patamia@unict.it (V.P.), chiara.zagni@unict.it (C.Z.), giuseppe.floresta@unict.it (G.F.), arescifina@unict.it (A.R.).

[2] Dipartimento di Scienze chimiche, Università di Catania, Viale A. Doria 6, 95125 Catania, Italy; roberto.fiorenza@unict.it (R.F.).

[3] IPCB-CNR, Via Paolo Gaifami 18; Institute for Polymers, Composites, and Biomaterials, Via Paolo Gaifami 18, 95126, Catania, Italy; sandro.dattilo@cnr.it (S.D.), paolomaria.riccobene@cnr.it (P.M.R.)

* Correspondence: giuseppe.floresta@unict.it (G.F.), arescifina@unict.it (A.R.)

Abstract: Nowadays, there is evidence that bacteria can contribute to cancer formation and interfere with therapy by mediating its carcinogenesis and related infection. Moreover, it is acknowledged that microbial infections and antibiotic resistance represent severe economic and health risks to society. These facts have led to the developing of several new techniques for impeding crucial biological processes in microbial cells. One of these techniques centers on using metal-chelating agents, which can disrupt the microorganism's vital metal metabolism by obstructing metal uptake and bioavailability for critical reactions. Additionally, nanotechnology has made a wide range of nanomaterials available for possible uses in the antibacterial industry. This complex field is shaped by antimicrobial nanoparticles, also investigated as therapeutic and drug-delivery tools. Halloysite nanotubes (HNTs) are naturally occurring tubular clay nanomaterials consisting of aluminosilicate kaolin sheets rolled up several times. The aluminon and siloxane groups on the surface of HNTs facilitate the formation of hydrogen bonds with biomaterials on their surface. These properties make HNTs crucial in a wide range of applications, such as in environmental sciences, wastewater treatment, dye removal, nanoelectronics and nanocomposite fabrication, catalytic studies, coatings for glass or anti-corrosive coatings, cosmetics, flame retardants, stimulus-response, and in forensic sciences. This work aimed to produce an antibacterial material by combining the properties of halloysite nanotubes with the ability of kojic acid to chelate iron. Starting from kojic acid, a simple nucleophilic substitution involving the hydroxyl groups on the surface of the nanotubes was performed. The obtained material was characterized by IR and SEM, and its ability to chelate iron was evaluated. Finally, the capacity to load drugs such as resveratrol and curcumin was also evaluated by UV analysis. In this way, a new bio-based material that can be used as a drug carrier and antimicrobial was produced.

Keywords: resveratrol; curcumin; halloysite nanotubes; kojic acid; iron chelation; antibacterial

1. Introduction

Millions of people die from cancer yearly, making it the world's most prominent cause of death [1]. Researchers are dedicated to examining the origins of cancer and its progression, associated treatments, and postoperative interventions. Since growing evidence shows that bacteria can contribute to cancer formation and interfere with therapy by mediating its carcinogenesis and related infection, bacteria, which initially appeared independent of cancer, have gained substantial interest among all cancer-related variables [2]. By triggering inflammatory responses and secreting bacterial enzymes, toxins, and oncogenic peptides, bacteria can make tumor growth worse. As bacteria may survive in malignant tissues due to the bacteria-friendly microenvironment and the severely immunocompromised function of patients, cancer patients are more likely to acquire bacterial

 doi:10.20944/preprints202306.0502.v1

infections after therapy [3]. In one study, patients with solid tumors had a 42% Gram-positive infection rate and 27% Gram-negative infection rate, compared to 47% and 30% for patients with hematological malignancies [4]. Moreover, surgery is frequently performed to remove most solid tumors, but this leaves scars or grafts at risk for infection, which can lead to inflammation, sluggish wound healing, and other consequences [5].

For example, the malignant tissue must be removed to treat skin cancer, but anti-infection and wound healing is challenging following surgery. Once an infection has set in, the delicate tissue will bleed, exude abundantly, cause discomfort, and cause fever—all of which are exceedingly harmful to cancer patients. The malignant bone is often replaced with an orthopedic implant in cases of bone tumor resection. The probable infection, however, may cause insufficient soft tissue covering, difficulties with the incision, and implant failure [2,6].

The need for antibacterial medications with novel or better modes of action is a health challenge of the highest relevance in the age of rising antimicrobial resistance [7]. One of the main methods to ensure progress seems to be to increase or enhance the chelating properties of already-existing medications or discover new, naturally-inspired chelating agents [8]. Resistance-based infections frequently do not respond to standard treatment, prolonging sickness, raising expenditures, and increasing the chance of mortality. Because the current antimicrobial medications either have too many adverse effects or tend to lose their efficacy due to the selection of resistant strains, the creation of innovative antimicrobial treatments is becoming more and more challenging [9].

These facts have led to the developing of several new techniques for impeding crucial biological processes in microbial cells. One such technique centers on using metal chelating agents, which can disrupt the metabolism of the metal vital to the microorganism, hindering metal uptake and bioavailability for critical reactions. [10].

The biological function of metal-dependent proteins, such as metalloproteases and transcription factors, can be inhibited by the chelation activity, which disturbs the homeostasis of microbial cells and blocks microbial nutrition, growth, and development, cellular differentiation, adhesion to biotic (such as extracellular matrix components, cell and/or tissue) and abiotic (such as plastic, silicone, and acrylic) structures, as well as the in vivo infection. Curiously, chelating drugs also increase the effectiveness of traditional antibacterial substances [5,10,11].

Nanomaterials have all the characteristics to address these problems and create new technologies that can effectively target bacterial infections. First, nanoscale particles' improved penetration and retention effect allows them to target tumor locations passively. Nanomaterials can be functionalized to actively target tumor tissues or cancer cells and accumulate at tumor sites through surface modification. For instance, cancer-targeting peptides can identify specific receptors [12–15], cationic elements can be added to nanomaterial surfaces to improve tumor penetrating ability [16], and nanomaterial shape or size can be altered to improve tumor retention. Second, nanomaterials' distinctive hydrophobic and hydrophilic architectures enable the loading of various medications in relatively high quantities, improving their solubility and safeguarding them against deterioration [17–19].

Natural clay nanotubes, known as halloysite, are one such nanoscale delivery method. It was discovered that halloysite is a practical and affordable nanoscale container for the encapsulation of physiologically active compounds, such as medicines and biocides [20,21]. The nearby alumina and silica layers, together with their water hydration, provide a packing disorder that causes the layers to roll up and bend, forming multilayer tubes [22]. Over other nanotubes, using a halloysite has several advantages. Production is neither laborious nor dangerous since it happens naturally. Compared to other nanotubes (such as carbon nanotubes and inorganic nanotubes composed of tungsten, titanium, etc.), it is less costly [23,24]. High particle size, many hydrophilic hydroxyl groups for functionalization, high stability in the biological fluid, and inexpensive cost are all benefits of HNTs for drug delivery carrier applications [25,26]. Halloysite nanotubes are harmless up to concentrations of 75 mg/mL, and parallel laser confocal observation of fluorescently labeled halloysite absorption of cells revealed the material's position inside the cells, close to the nucleus, demonstrating cellular uptake [25].

 doi:10.20944/preprints202306.0502.v1

In this work, we have modified HNTs with a derivative of kojic acid and then encapsulated them with resveratrol and curcumin, natural phenolic compounds with many beneficial effects on human health, such as antioxidant, anticancer, neuroprotective, and antiviral activity [27–29]. The successful preparation of this material was confirmed by various characterization methods. The novel material proved excellent drug loading efficiency and chelating properties as proof of concept of a dual-acting antibacterial nanomaterial with resveratrol/curcumin and iron depletion properties.

2. Materials and Methods

2.1. Materials

All the required chemicals were purchased from Merck and used without further purification. ^{1}H- and ^{13}C-NMR spectra were recorded at 300 K on Varian UNITY Inova using DMSO-d_6 as the solvent at 500 MHz for ^{1}H-NMR and 125 MHz for ^{13}C-NMR.

2.2. Synthesis of HNTs

2.2.1. Synthesis of Chlorokojic Acid 2

In a 100 mL round bottom reaction flask containing freshly distilled thionyl chloride (20 mL), kojic acid **1** (7.3g) was added, and the mixture was magnetically stirred for 2 h. After one hour, a yellow-to-orange precipitate is formed. The product is collected by filtration, washed with petroleum ether, and then recrystallized from water to give colorless needles of chlorokojic acid **2** (5.2 g) in 63% yield. The ^{1}H and ^{13}C NMR of the compound were accordingly to the literature [30].

2.2.2. Synthesis of HNTs/Kojic Acid Derivative

In a 10 mL round bottom reaction flask containing DMF (2 mL) was added halloysite (400 mg, 1 eq, 1.36 mmol) and triethylamine (1.14 mL, 6 eq, 8.16 mmol), and the mixture was magnetically stirred at room temperature for 30 minutes. Subsequently, chlorokojic acid (437 mg, 2 eq, 2.72 mmol) was added, and the reaction mixture was left to stir overnight at 80 °C. Then, the precipitate was collected by filtration, washed with acetone several times (5 × 10 mL), and thus placed in an oven at 65 °C overnight to obtain the final product (470 mg) in 60% yield.

2.3. IR and UV-vis

FTIR analyses in the 4000–400 cm^{-1} region were obtained using an FTIR System 2000 (Perkin-Elmer, Waltham, MA, USA) with KBr as the medium. The Drug Loading Capacity (DLC) and Encapsulation Efficiency (EE) were evaluated using the spectrophotometric UV-vis method with a JASCO V-730 instrument.

2.4. Resveratrol and Curcumin Uptake

Resveratrol charge on the HNTs-kojic system was carried, according to the literature [31,32], on at different weight ratios: 1:1, 1:2.5, 1:5, and 1:10 (resveratrol:HNTs-kojic w/w, Figure 1). Briefly, resveratrol solution in water was prepared (7.5 mg L^{-1}), and the correct amount of HNTs-kojic was suspended and kept under stirring for 1 h in the dark. Then, the suspension was centrifuged to separate the system from the uncharged drug. The loading capacities of curcumin were also evaluated, using different w/w ratios between the drug and HNTs-kojic system. According to the literature [33], a stock solution in ethanol was prepared (0.663 mg L^{-1}), and curcumin was charged on the HNTs-kojic system employing different weight ratios: 1:10, 1:50, 1:100, and 1:1000 (curcumin:HNTs-kojic w/w, Figure 2).

Preprints (www.preprints.org) | NOT PEER-REVIEWED | Posted: 7 June 2023 doi:10.20944/preprints202306.0502.v1

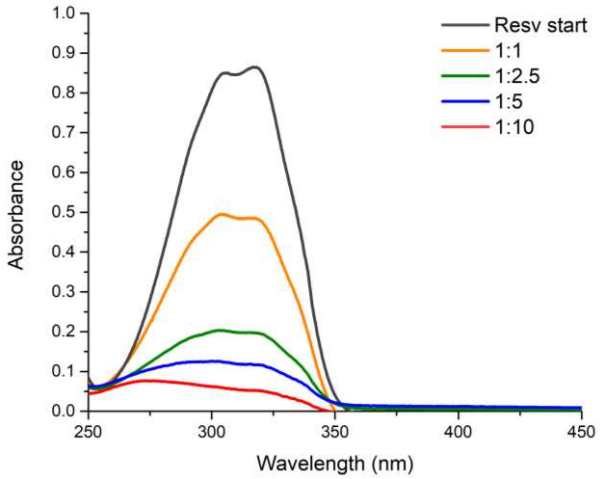

Figure 1. UV spectra of the loading capacity of resveratrol on the HNTs-kojic system with different ratios.

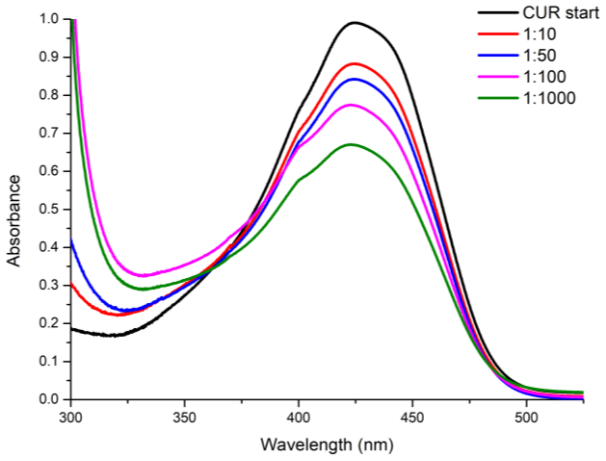

Figure 2. UV spectra of the loading capacity of curcumin on the HNTs-kojic system with different ratios.

2.5. ICP/MS

Quantitative determination of iron ions in solution was performed by an inductively coupled plasma–mass spectrometry (ICP/MS) Nexion 300X (Perkin Elmer Inc. Waltham, Massachusetts, USA.) instrument using the kinetic energy discrimination (KED) for interference suppression. Each determination was performed three times. The accuracy of the analytical procedure was confirmed by measuring a standard reference material, Nist 1640a trace element in natural water, without observing an appreciable difference.

Batch equilibrium tests were carried out to calculate the metal ions removal percentage. In general, 10 mg of HNTs-kojic were immersed into iron(III) chloride ($FeCl_3$) solutions (5 mL and pH = 6) at different initial concentrations of 1.50 and 10.00 mg L^{-1} as Fe content. The vials were maintained under constant shaking at 25 °C and 180 rpm for 24 h, the suspension obtained was filtrated throw a 0.22 nylon filter, and the solution was subjected to analysis by ICP-MS as previously described.

2.6. SEM and EDX

Scanning electron microscopy (SEM) Phenomenex microscope was used to study the morphology of the synthesized material. To increase conductivity before the test, samples were pre-coated with gold sputter coating. Images were then captured to examine the nanoclay morphology of the sample. The data were acquired and processed using Phenom Porometric 1.1.2.0 (Phenom-

Preprints (www.preprints.org) | NOT PEER-REVIEWED | Posted: 7 June 2023 doi:10.20944/preprints202306.0502.v1

World BV, Eindhoven, The Netherlands). Energy-dispersive X-ray spectroscopy (EDX) was used to analyze the chemical elements material and determine its chemical composition.

3. Results and discussion

To produce a derivative able to react with the hydroxylic groups of the HNTs nanotubes, a derivative of kojic acid (**1**) was produced, giving chlorokojic acid (**2**) by simple reaction with thionyl chloride (Figure 3). Compound **2** was then reacted with the HNTs, as reported in Figure 4, giving the final product **3**, named HNTs-kojic. Considering the obtained quantity of HNTs-kojic (470 mg) and the displacement of the chlorine, a final functionalization of 1.4 mmol/g (45%) can be calculated.

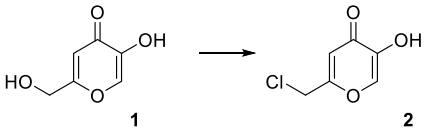

Figure 3. Synthesis of compound **2**.

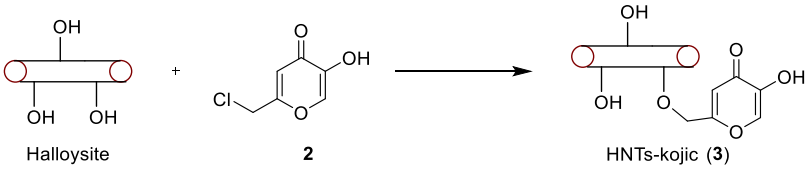

Figure 4. Synthesis of compound **3**.

Therefore, the material was characterized employing IR, ICP/MS, SEM, EDX, and the drug delivery capabilities were proven by the drug loading UV experiments of two natural molecules with antibacterial properties, resveratrol and curcumin [34-36].

The comparison of the IR spectra of HNTs and HNTs-kojic shows the successful functionalization of the halloysite nanotubes with kojic acid (Figure 5). In the spectrum of HNTs (red line), bands related to the OH groups are evident: the peak at 906 cm^{-1} is attributable to the Al-O-OH vibration, while the bands at 3695 and 3620 cm^{-1} are attributed to the stretching vibration of the Al-OH groups. In addition, a strong peak related to O-Si-O is observed at around 1075 cm^{-1}, and the peaks at 793 and 752 cm^{-1} can be assigned to the stretching mode of apical Si-O [31].

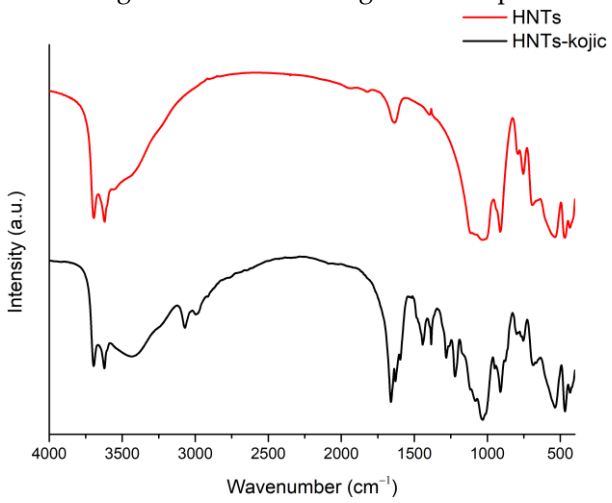

Figure 5. IR spectra of pristine halloysite (red line) and halloysite functionalized with kojic acid (black line).

From the spectrum related to the functionalized HNTs-kojic (black line), it is evident the presence of signals related to halloysite nanotubes along with typical kojic acid signals: at 2985 and 3070 cm^{-1} the medium stretching of CH_2 [37]; at 1659 cm^{-1} a strong signal related to conjugated ketone C=O; at 1627 cm^{-1} the stretching of C=C typical of an unsaturated ketone [38,39]; and finally the

Preprints (www.preprints.org) | NOT PEER-REVIEWED | Posted: 7 June 2023 doi:10.20944/preprints202306.0502.v1

stretching related to C-O at 1219 cm^{-1}, which highlights the successful functionalization between the nanotube and kojic acid.

ICP-MS spectra were conducted to verify the ability of the material to sequestrate iron(III) from the environment. The experiments revealed that HNTs-kojic chelate iron, i.e., eliminate gallium from solutions with 65.33% retention of the ion when working at 1.50 mg/L of iron chloride and 10.08% retention of the ion when working at 10.00 mg/L.

Figure 6 shows SEM images obtained from HNTs-kojic spread on a flat support. SEM observation confirmed the presence of pure and functionalized HNT, as most of the sample consists of cylindrical tubes [40].

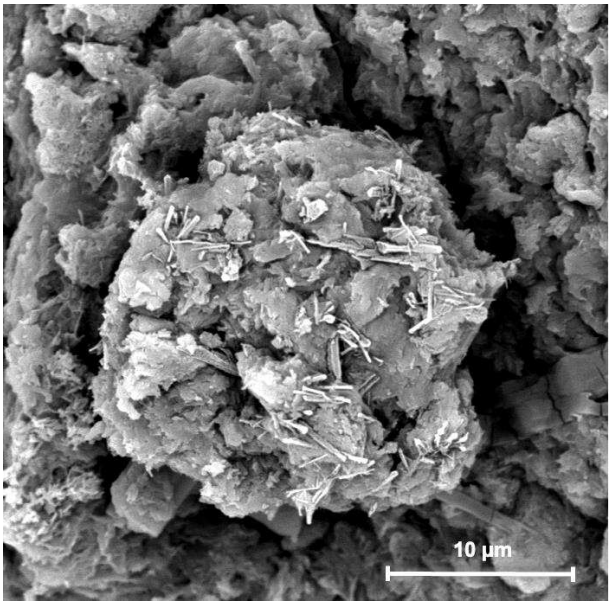

Figure 6. SEM image of HNTs-kojic.

The SEM-EDX elemental mapping of surface-modified HNTs-kojic is shown in Figure 7. The major constituents of HNT are oxygen, aluminum, and silicon. The HNTs-kojic shows the presence of carbon and oxygen, silicon, and aluminum.

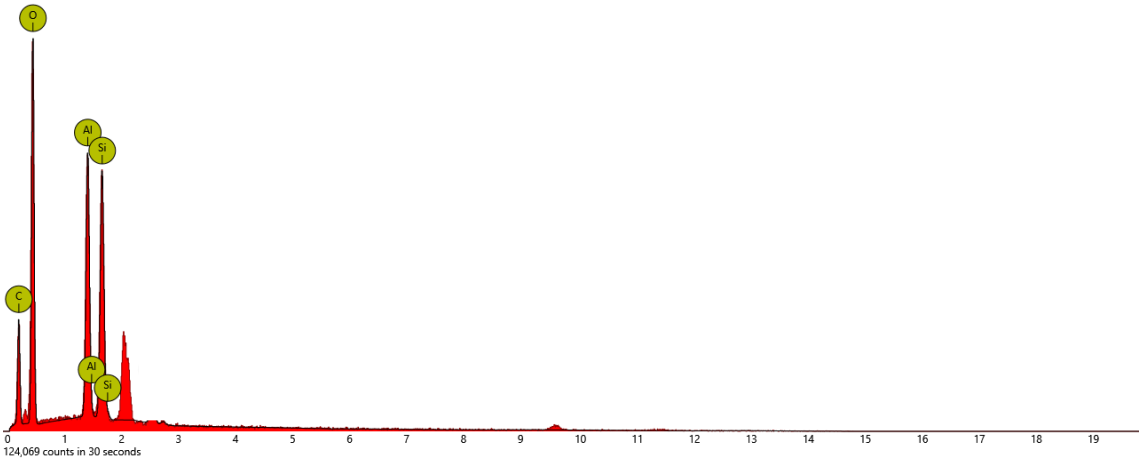

Figure 7. EDX of HNTs-kojic. In ordinate the counts, whereas as abscissa the keV. The unlabelled peaks at 2.1 and 9.6 keV correspond to gold, which is used to confer conductivity.

Table 2. Atomic and weight concentration from EDX analysis of HNTs-kojic.

Element Symbol	Atomic Conc.	Weight Conc.
O	45.27	45.06
C	40.70	30.41

Preprints (www.preprints.org) | NOT PEER-REVIEWED | Posted: 7 June 2023 doi:10.20944/preprints202306.0502.v1

Al	6.76	11.35
Si	6.22	10.87

The Drug Loading Capacity (DLC) and Encapsulation Efficiency (EE) were evaluated using the spectrophotometric UV-vis method with a JASCO V-730 instrument. The DLC and the EE were evaluated following Equations (1) and (2), respectively [31,41]:

$$DLC = \frac{loaded\ drug\ amount}{total\ loofah\ amount} \quad (1)$$

$$EE = \frac{loaded\ drug\ amount}{total\ drug\ amount} \quad (2)$$

From Figure 8, it is possible to note that the highest EE was obtained with the highest quantity of adsorbent, as expected. However, it is more suitable for our purpose to evaluate the DLC that is optimized with a 1:1 drug-adsorbent ratio. The results obtained align with the data reported in the literature for the delivery of resveratrol [31]. The same experiments were conducted with curcumin; once again, the DLC and EE values (Figure 9) detected by UV analysis were in excellent agreement with the literature [33,42,43].

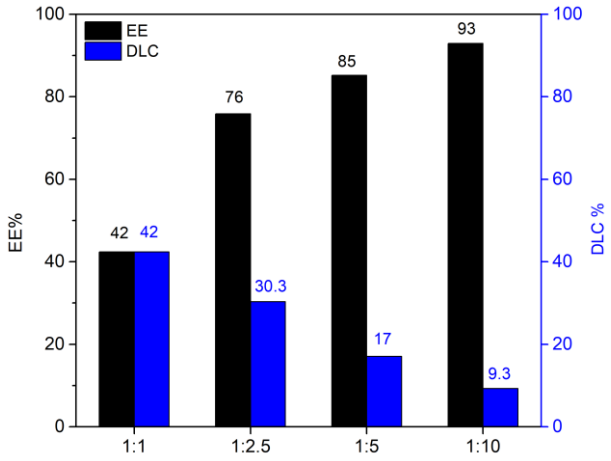

Figure 8. Encapsulation efficiency (EE) and drug loading capacity (DLC) of resveratrol on the HNTs-kojic.

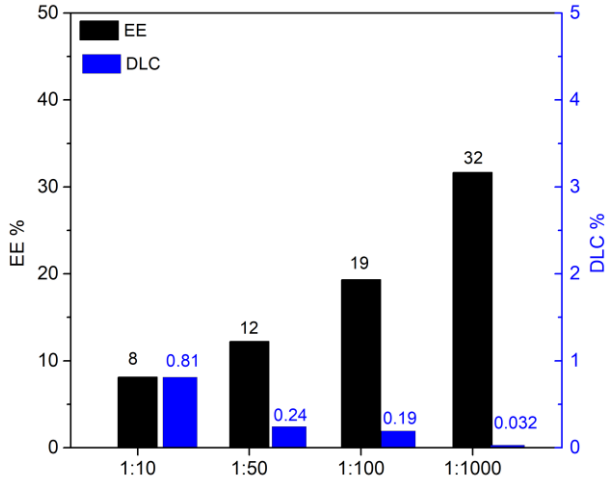

Figure 9. Encapsulation efficiency (EE) and drug loading capacity (DLC) of curcumin on the HNTs-kojic.

4. Conclusions

The use of antibiotics in cancer therapy has advanced significantly, especially with the rapid development of nanomedicine. Significant efforts have been made to build nanosystems to improve the efficacy of medication delivery, adopt novel therapeutic agents or treatment modalities to reduce drug resistance and implement local antimicrobial therapy. Nevertheless, there are always new difficulties associated with new approaches. The size and surface charge of nanocarriers are crucial because they can affect nanoparticle detection, adsorption, and removal, influencing how widely distributed they are throughout the body. Even after they have reached the tumor site, smaller-scale nanoparticles in the circulatory system can be quickly cleared and leaked back into the circulation, whereas larger nanoparticles have strong retention but are unable to penetrate cells.

Antibacterial nanosystems have made impressive advancements in cancer therapy overall, but there is still more work to be done before they can be used effectively and safely [44,45]. Because of high biocompatibility and on-demand drug delivery HNTs have received much interest recently in the biomedical area; by adding the appropriate chemotherapy or antibacterial medications HNTs can be employed for antitumor or antibacterial treatment as well as for the treatment of other diseases [26].

This work proposed the synthesis of a new nanomaterial based on HNTs and kojic acid (HNTs-kojic). HNTs-kojic was characterized by several techniques, and its iron chelation as well as its drug delivery capabilities, have been well documented.

The system has been developed to serve as a proof of concept of a dual-acting antibacterial nanomaterial with resveratrol/curcumin and iron depletion properties for cancer and other infection-related applications. The chelating moiety of maltol was chemically bonded to the material, and the resveratrol/curcumin was incorporated into the HNTs cavity.

This new material proved that applying the dual action due to the drug and the iron chelating properties is possible in a HNTs. These findings would open the way for further research and applications of the developed material in cancer treatment and other infections-related issues. Even if the use of HNTs in the treatment of tumors is still in the experimental stage, this new prototype material can have a wide range of applications in cancer and other fields, e.g., using HNTs-kojic with the already studied molecules, i.e., resveratrol or curcumin using HNTs-kojic as a drug carrier for other molecules (antibacterial or others) – reevaluation/potentiation of old antibiotics – combined use of the solutions mentioned. Experimental antibacterial evaluations of HNTs-kojic are ongoing in our laboratory, and we will follow up with this publication.

Supplementary Materials: The following supporting information can be downloaded at: www.mdpi.com/xxx/s1, Figure S1: title; Table S1: title; Video S1: title.

Author Contributions: Conceptualization, G.F. and V.P.; methodology, G.F., V.P., C.Z., R.F. and S.D.; validation, G.F., V.P., C.Z., R.F.; investigation, G.F. and V.P.; resources, R.F., S.D., P.M.R. and A.R.; data curation, V.P., C.Z., R.F., P.M.R. and S.D.; writing—original draft preparation, G.F., V.P. and C.Z.; writing—review and editing, G.F. and A.R.; visualization, V.P. and C.Z.; supervision, V.P., G.F. and A.R.; project administration, G.F. and A.R., funding acquisition, A.R. All authors have read and agreed to the published version of the manuscript.

Funding: The research leading to these results has received funding from the European Union—NextGenerationEU through the Italian Ministry of University and Research under PNRR—M4C2-I1.3 Project PE_00000019 "HEAL ITALIA" (Antonio Rescifina and Vincenzo Patamia), CUP E63C22002080006. The views and opinions expressed are those of the authors only and do not necessarily reflect those of the European Union or the European Commission. Neither the European Union nor the European Commission can be held responsible for them.

Data Availability Statement: Not applicable.

Acknowledgments: Not applicable.

Conflicts of Interest: The authors declare no conflict of interest.

References

1. Siegel, R.L.; Miller, K.D.; Fuchs, H.E.; Jemal, A. Cancer statistics, 2022. *CA Cancer J Clin* **2022**, *72*, 7-33, doi:10.3322/caac.21708.
2. Rao, J.; Yang, Y.; Pan Bei, H.; Tang, C.-Y.; Zhao, X. Antibacterial nanosystems for cancer therapy. *Biomaterials Science* **2020**, *8*, 6814-6824, doi:10.1039/D0BM01537G.
3. Xiao, L.; Zhang, Q.; Peng, Y.; Wang, D.; Liu, Y. The effect of periodontal bacteria infection on incidence and prognosis of cancer: A systematic review and meta-analysis. *Medicine (Baltimore)* **2020**, *99*, e19698, doi:10.1097/MD.0000000000019698.
4. Yadegarynia, D.; Tarrand, J.; Raad, I.; Rolston, K. Current spectrum of bacterial infections in patients with cancer. *Clin Infect Dis* **2003**, *37*, 1144-1145, doi:10.1086/378305.
5. Simões, D.; Miguel, S.P.; Ribeiro, M.P.; Coutinho, P.; Mendonça, A.G.; Correia, I.J. Recent advances on antimicrobial wound dressing: A review. *Eur J Pharm Biopharm* **2018**, *127*, 130-141, doi:10.1016/j.ejpb.2018.02.022.
6. Lascelles, B.D.; Dernell, W.S.; Correa, M.T.; Lafferty, M.; Devitt, C.M.; Kuntz, C.A.; Straw, R.C.; Withrow, S.J. Improved survival associated with postoperative wound infection in dogs treated with limb-salvage surgery for osteosarcoma. *Ann Surg Oncol* **2005**, *12*, 1073-1083, doi:10.1245/aso.2005.01.011.
7. Saha, M.; Sarkar, A. Review on Multiple Facets of Drug Resistance: A Rising Challenge in the 21st Century. *J Xenobiot* **2021**, *11*, 197-214, doi:10.3390/jox11040013.
8. Repac Antić, D.; Parčina, M.; Gobin, I.; Petković Didović, M. Chelation in Antibacterial Drugs: From Nitroxoline to Cefiderocol and Beyond. *Antibiotics* **2022**, *11*, doi:10.3390/antibiotics11081105.
9. Boyd, N.K.; Teng, C.; Frei, C.R. Brief Overview of Approaches and Challenges in New Antibiotic Development: A Focus On Drug Repurposing. *Front Cell Infect Microbiol* **2021**, *11*, 684515, doi:10.3389/fcimb.2021.684515.
10. Santos, A.L.; Sodre, C.L.; Valle, R.S.; Silva, B.A.; Abi-Chacra, E.A.; Silva, L.V.; Souza-Goncalves, A.L.; Sangenito, L.S.; Goncalves, D.S.; Souza, L.O.; et al. Antimicrobial action of chelating agents: repercussions on the microorganism development, virulence and pathogenesis. *Curr Med Chem* **2012**, *19*, 2715-2737, doi:10.2174/092986712800609788.
11. Ghanem, S.; Kim, C.J.; Dutta, D.; Salifu, M.; Lim, S.H. Antimicrobial therapy during cancer treatment: Beyond antibacterial effects. *J Intern Med* **2021**, *290*, 40-56, doi:10.1111/joim.13238.
12. Floresta, G.; Abbate, V. Recent progress in the imaging of c-Met aberrant cancers with positron emission tomography. *Med Res Rev* **2022**, *42*, 1588-1606, doi:10.1002/med.21885.
13. Floresta, G.; Memdouh, S.; Pham, T.; Ma, M.T.; Blower, P.J.; Hider, R.C.; Abbate, V.; Cilibrizzi, A. Targeting integrin αvβ6 with gallium-68 tris (hydroxypyridinone) based PET probes. *Dalton Transactions* **2022**, *51*, 12796-12803, doi:10.1039/D2DT00980C.
14. Failla, M.; Floresta, G.; Abbate, V. Peptide-based positron emission tomography probes: current strategies for synthesis and radiolabelling. *RSC Medicinal Chemistry* **2023**, doi:10.1039/D2MD00397J.
15. Floresta, G.; Keeling, G.P.; Memdouh, S.; Meszaros, L.K.; de Rosales, R.T.M.; Abbate, V. NHS-Functionalized THP Derivative for Efficient Synthesis of Kit-Based Precursors for 68Ga Labeled PET Probes. *Biomedicines* **2021**, *9*, doi:10.3390/biomedicines9040367.
16. Cilibrizzi, A.; Pourzand, C.; Abbate, V.; Reelfs, O.; Versari, L.; Floresta, G.; Hider, R. The synthesis and properties of mitochondrial targeted iron chelators. *Biometals* **2022**, doi:10.1007/s10534-022-00383-8.
17. Fang, X.; Wang, C.; Zhou, S.; Cui, P.; Hu, H.; Ni, X.; Jiang, P.; Wang, J. Hydrogels for Antitumor and Antibacterial Therapy. *Gels* **2022**, *8*, doi:10.3390/gels8050315.
18. Zagni, C.; Coco, A.; Patamia, V.; Floresta, G.; Curcuruto, G.; Mangano, K.; Mecca, T.; Rescifina, A.; Carroccio, S. Cyclodextrin-Based Cryogels for Controlled Drug Delivery. *Medical Sciences Forum* **2022**, *14*, doi:10.3390/ECMC2022-13449.
19. Zagni, C.; Dattilo, S.; Mecca, T.; Gugliuzzo, C.; Scamporrino, A.A.; Privitera, V.; Puglisi, R.; Carola Carroccio, S. Single and dual polymeric sponges for emerging pollutants removal. *European Polymer Journal* **2022**, *179*, 111556, doi:https://doi.org/10.1016/j.eurpolymj.2022.111556.
20. Zagni, C.; Scamporrino, A.A.; Riccobene, P.M.; Floresta, G.; Patamia, V.; Rescifina, A.; Carroccio, S.C. Portable Nanocomposite System for Wound Healing in Space. *Nanomaterials (Basel)* **2023**, *13*, doi:10.3390/nano13040741.
21. Price, R.R.; Gaber, B.P.; Lvov, Y. In-vitro release characteristics of tetracycline HCl, khellin and nicotinamide adenine dineculeotide from halloysite; a cylindrical mineral. *J Microencapsul* **2001**, *18*, 713-722, doi:10.1080/02652040010019532.
22. Lvov, Y.M.; Shchukin, D.G.; Möhwald, H.; Price, R.R. Halloysite clay nanotubes for controlled release of protective agents. *ACS Nano* **2008**, *2*, 814-820, doi:10.1021/nn800259q.
23. Hasani, M.; Abdouss, M.; Shojaei, S. Nanocontainers for drug delivery systems: A review of Halloysite nanotubes and their properties. *Int J Artif Organs* **2021**, *44*, 426-433, doi:10.1177/0391398820968836.

24. Jha, R.; Singh, A.; Sharma, P.K.; Fuloria, N.K. Smart carbon nanotubes for drug delivery system: A comprehensive study. *Journal of Drug Delivery Science and Technology* **2020**, *58*, 101811, doi:https://doi.org/10.1016/j.jddst.2020.101811.
25. Vergaro, V.; Lvov, Y.M.; Leporatti, S. Halloysite clay nanotubes for resveratrol delivery to cancer cells. *Macromol Biosci* **2012**, *12*, 1265-1271, doi:10.1002/mabi.201200121.
26. Biddeci, G.; Spinelli, G.; Colomba, P.; Di Blasi, F. Nanomaterials: A Review about Halloysite Nanotubes, Properties, and Application in the Biological Field. *International Journal of Molecular Sciences* **2022**, *23*, doi:10.3390/ijms231911518.
27. Giordano, A.; Tommonaro, G. Curcumin and Cancer. *Nutrients* **2019**, *11*, doi:10.3390/nu11102376.
28. Brisdelli, F.; D'Andrea, G.; Bozzi, A. Resveratrol: a natural polyphenol with multiple chemopreventive properties. *Curr Drug Metab* **2009**, *10*, 530-546, doi:10.2174/138920009789375423.
29. Gülçin, İ. Antioxidant properties of resveratrol: A structure–activity insight. *Innovative Food Science & Emerging Technologies* **2010**, *11*, 210-218, doi:https://doi.org/10.1016/j.ifset.2009.07.002.
30. Ma, Y.; Luo, W.; Quinn, P.J.; Liu, Z.; Hider, R.C. Design, Synthesis, Physicochemical Properties, and Evaluation of Novel Iron Chelators with Fluorescent Sensors. *Journal of Medicinal Chemistry* **2004**, *47*, 6349-6362, doi:10.1021/jm049751s.
31. Patamia, V.; Fiorenza, R.; Brullo, I.; Zambito Marsala, M.; Balsamo, S.A.; Distefano, A.; Furneri, P.M.; Barbera, V.; Scirè, S.; Rescifina, A. A sustainable porous composite material based on loofah-halloysite for gas adsorption and drug delivery. *Materials Chemistry Frontiers* **2022**, *6*, 2233-2243, doi:10.1039/D2QM00505K.
32. Vergaro, V.; Lvov, Y.M.; Leporatti, S. Halloysite Clay Nanotubes for Resveratrol Delivery to Cancer Cells. *Macromolecular Bioscience* **2012**, *12*, 1265-1271, doi:https://doi.org/10.1002/mabi.201200121.
33. Dionisi, C.; Hanafy, N.; Nobile, C.; Giorgi, M.L.D.; Rinaldi, R.; Casciaro, S.; Lvov, Y.M.; Leporatti, S. Halloysite Clay Nanotubes as Carriers for Curcumin: Characterization and Application. *IEEE Transactions on Nanotechnology* **2016**, *15*, 720-724, doi:10.1109/TNANO.2016.2524072.
34. Vestergaard, M.; Ingmer, H. Antibacterial and antifungal properties of resveratrol. *International Journal of Antimicrobial Agents* **2019**, *53*, 716-723, doi:https://doi.org/10.1016/j.ijantimicag.2019.02.015.
35. Moghadamtousi, S.Z.; Kadir, H.A.; Hassandarvish, P.; Tajik, H.; Abubakar, S.; Zandi, K. A review on antibacterial, antiviral, and antifungal activity of curcumin. *Biomed Res Int* **2014**, *2014*, 186864, doi:10.1155/2014/186864.
36. Munir, Z.; Banche, G.; Cavallo, L.; Mandras, N.; Roana, J.; Pertusio, R.; Ficiarà, E.; Cavalli, R.; Guiot, C. Exploitation of the Antibacterial Properties of Photoactivated Curcumin as ‘Green’ Tool for Food Preservation. *International Journal of Molecular Sciences* **2022**, *23*, doi:10.3390/ijms23052600.
37. Patamia, V.; Tomarchio, R.; Fiorenza, R.; Zagni, C.; Scirè, S.; Floresta, G.; Rescifina, A. Carbamoyl-Decorated Cyclodextrins for Carbon Dioxide Adsorption. *Catalysts* **2023**, *13*, doi:10.3390/catal13010041.
38. Baharfar, R.; Alinezhad, H.; Azimi, R. Use of DABCO-functionalized mesoporous SBA-15 as catalyst for efficient synthesis of kojic acid derivatives, potential antioxidants. *Research on Chemical Intermediates* **2015**, *41*, 8637-8650, doi:10.1007/s11164-014-1916-y.
39. Andrade, G.F.; Lima, G.d.S.; Gastelois, P.L.; Assis Gomes, D.; Macedo, W.A.d.A.; de Sousa, E.M.B. Surface modification and biological evaluation of kojic acid/silica nanoparticles as platforms for biomedical systems. *International Journal of Applied Ceramic Technology* **2020**, *17*, 380-391, doi:https://doi.org/10.1111/ijac.13376.
40. Murphy, Z.; Kent, M.; Freeman, C.; Landge, S.; Koricho, E. Halloysite nanotubes functionalized with epoxy and thiol organosilane groups to improve fracture toughness in nanocomposites. *SN Applied Sciences* **2020**, *2*, 2130, doi:10.1007/s42452-020-03909-2.
41. Zhao, Y.; Cai, C.; Liu, M.; Zhao, Y.; Wu, Y.; Fan, Z.; Ding, Z.; Zhang, H.; Wang, Z.; Han, J. Drug-binding albumins forming stabilized nanoparticles for co-delivery of paclitaxel and resveratrol: In vitro/in vivo evaluation and binding properties investigation. *International Journal of Biological Macromolecules* **2020**, *153*, 873-882, doi:https://doi.org/10.1016/j.ijbiomac.2020.03.060.
42. Liu, M.; Chang, Y.; Yang, J.; You, Y.; He, R.; Chen, T.; Zhou, C. Functionalized halloysite nanotube by chitosan grafting for drug delivery of curcumin to achieve enhanced anticancer efficacy. *Journal of Materials Chemistry B* **2016**, *4*, 2253-2263, doi:10.1039/C5TB02725J.
43. Rao, K.M.; Kumar, A.; Suneetha, M.; Han, S.S. pH and near-infrared active; chitosan-coated halloysite nanotubes loaded with curcumin-Au hybrid nanoparticles for cancer drug delivery. *International Journal of Biological Macromolecules* **2018**, *112*, 119-125, doi:https://doi.org/10.1016/j.ijbiomac.2018.01.163.
44. Tiwari, S.; Juneja, S.; Ghosal, A.; Bandara, N.; Khan, R.; Wallen, S.L.; Ramakrishna, S.; Kaushik, A. Antibacterial and antiviral high-performance nanosystems to mitigate new SARS-CoV-2 variants of concern. *Curr Opin Biomed Eng* **2022**, *21*, 100363, doi:10.1016/j.cobme.2021.100363.
45. Ermini, M.L.; Voliani, V. Antimicrobial Nano-Agents: The Copper Age. *ACS Nano* **2021**, *15*, 6008-6029, doi:10.1021/acsnano.0c10756.

 doi:10.20944/preprints202306.0502.v1